THE POSITRONIUM RADIATIVE COMBINATION SPECTRUM: CALCULATION IN THE LIMIT OF THERMAL POSITRONS AND LOW DENSITIES

P. Wallyn and W. A. Mahoney

Jet Propulsion Laboratory 169-327, California Institute of Technology
4800 Oak Grove Drive, Pasadena, CA 91109 USA.

and

Ph. Durouchoux and C. Chapuis

DAPNIA, M-vice d'Astrophysique, CE Saclay
91191 Gif sur Yvette Cedex, France.

to be published in *The Astrophysical Journal*

ABSTRACT

We calculate the intensities of the positronium de-excitation lines for two processes: (i), the radiative combination of free thermal electrons and positrons for transitions with principal quantum number $n \leq 20$ and (ii) charge exchange between free positrons and hydrogen and helium atoms, restricting our evaluation to the Lyman-et line. We consider a low density medium modeled by the case A assumption of Baker and Menzel (1938) and use the "nL method" of Pengelly (1964) to calculate the absolute intensities. We also evaluate the positronium fine and hyperfine intensities and show that these transitions are in all cases much weaker than positronium de-excitation lines in the same wavelength range. We also extrapolate our positronium de-excitation intensities to the submillimeter, millimeter and centimeter wavelengths. Our results favor the search of infrared transitions of positronium lines for point sources when the visual extinction A_v is greater than -5.

Subject headings: atomic processes __elementary particles __line: formation__ Galaxy: center

1 INTRODUCTION

The de-excitation lines produced when a positron and an electron combine to form positronium (Ps) in an excited state represent a promising way to detect annihilation sites in space (Table 1). Since the idea of searching for Ps de-excitation lines in stellar spectra by Mohorovicic (1934), no detection has ever been made in astrophysical objects and only laboratory measurements provided spectra of the Lyα λ2430 line (Canter et al. 1975). Nevertheless, two unsuccessful searches for Ps de-excitation lines, in the direction of the Galactic center (GC) at radio and millimeter wavelengths, have so far been published: the first one, in the direction of SgrA

(Anantharamaiah et al. 1989), searching for Ps87α, Ps89α, Ps129α and Ps133α with the Very Large Army (VLA) and Ps32α with the IRAM 30-m telescope. The second (Anantharamaiah et al. 1993) considered the famous gamma-ray source and positron emitter 1E1740.7-2942, searching for Ps 87α with the VLA. The Lyman series of Ps has been searched by Burdyuzha et al. (1987) in the UV spectra of SN 1987 A without positive detection. Fine-structure transitions of positronium from level n = 2 have been investigated in laboratory (Mills et al. 1975, Hagena et al. 1993). The 1^3S_1-2^3S_1 transition has also been observed for the first time by Chu and Mills (1982) using two-photon Doppler free excitation (Table 2). Detection of the ground state hyperfine splitting 1^3S_1-1^1S_0 at 1.47 mm has been done in laboratory by Deutsch (1951) but its detection in the GC direction was unsuccessful (Encrenaz, private communication).

The principal work on the detection of Ps de-excitation lines in astrophysical sites has been done by McClintock (1984) who analyzed the Lyα λ2430 line formation in ionized media during the radiative combination of free thermal electron-positron pairs. The author gives evaluations of the intensity of the Lyα transition of Ps for various positron sources (GC, Crab nebula, etc..), assuming that the Ps excited states have the same relative probabilities as hydrogen atom recombination lines and neglecting any absorption mechanism. We consider in this paper the Ps line width and intensity for two Ps formation processes: (i) radiative combination in a plasma of free electrons and positrons and (ii) charge exchange between thermal positrons and H and He atoms, the most abundant species in the interstellar medium. In both cases we will neglect collisions of Ps atoms with other particles and phenomena including non thermal positron populations.

We introduce calculations of radiative electron-positron combination in §2 and investigate charge exchange processes with H and He in low levels quantum states in §3. The method we use to model de-excitation lines from Ps is presented in §4, emphasizing at each step the variations with the electron radiative recombination process on protons. We then give in §5 evaluations of Ps line intensities in a large interval of temperatures for principal quantum states up to n = *20* and we also estimate Ps line intensies for Ps32α, Ps87α, Ps89α, Ps129α, Ps133α and fine and hyperfine line intensities fo, transitions to the ground and first excited state and conclude this study by comparing the luminosity flux expected from a point source in the GC region for different Ps transitions in order to identify the best stategy for future observations.

2 ELECTRON-POSITRON RADIATIVE COMBINATION

Stobbe (1930) was the first to calculate accurate Ps combination cross sections based on Gordon (1929) radial matrix elements. Nieminen (1967) emphasized these works and calculated the cross section behaviour in the limit of high quantum levels and pointed out the inaccuracy of the Born approximation. Gould (1989), calculated radiative combination reaction rates from first principles for both Ps ground and total excited states, More recently, Burdyuzha et al. (1992) published formulae of combination cross sections for positronium of quantum states up to n = 3 based on the Stobbe (1930) paper and pointed out the role of Ps collisions. Their calculations have been pursued for low energy positrons (Burdyuzha and Kauts 1994) giving results in good agreement with Nieminen (1967).

We use here the calculations of Stobbe (1930) valid for non-relativistic electron-positron pairs (the error for pairs of relative kinetic energy of 680 eV is about 1%, Nieminen 1967). In units where $\hbar = c = G = 1$, the cross section for positronium formation in a state with quantum numbers n and L is given by (Nieminen 1967):

$$\sigma_{nL} = \frac{16\pi\alpha\omega^3}{3v}\left[(L+1)(C_{nL}^{L+1})^2 + L\,(C_{nL}^{L-1})^2\right] \qquad (2.1)$$

with the radial matrix elements:

$$C_{nL}^{L+1} = \frac{(-1)^{n+L+1}2^{2L+4}\sqrt{2\pi}}{\alpha m^{5/2}v^{3/2}(2L+1)!}\sqrt{\frac{(n+L)!\,\prod_{s=0}^{L+1}(s^2+(\frac{\alpha}{v})^2)}{(n-L-1)!\,\sinh(\frac{\pi\alpha}{v})}}\; e^{\frac{\alpha}{v}\left(2\ \frac{\pi}{\chi}-\ \frac{2}{\chi}\right)}\frac{\arctan(\frac{1}{\chi})}{(1+\chi^2)^n}$$

$$\times \mathrm{Im}\left[(\chi-i)^{2n-2L-4}\, F\left(L+2+\frac{i\alpha}{v};\, L+1-n;\, 2L+2;\, \frac{-4i\chi}{(\chi-i)^2}\right)\right] \tag{2.2}$$

and:

$$C_{nl}^{L-1} = \frac{(-1)^{n+L}2^{2L+1}\sqrt{2\pi}}{\alpha m^{5/2}v^{3/2}(2L-1)!}\sqrt{\frac{(n+L)!\prod_{s=0}^{L-1}(s^2+(\frac{\alpha}{v})^2)}{(n-L-1)!\,\sinh(\frac{\pi\alpha}{v})}}\; e^{\frac{\alpha}{v}\left(\frac{\pi}{2}-2\,\mathrm{arctg}(\frac{1}{\chi})\right)}\left(\frac{\chi}{(1+\chi^2)}\right)^{L+1}$$

$$\times\left[\left(\frac{\chi-i}{\chi+i}\right)^{n-L-1} F\left(L+\frac{i\alpha}{v};\, L-tI-n;\, 2L;\, \frac{-4i\chi}{(\chi-i)^2}\right) - \left(\frac{\chi-i}{\chi+i}\right)^{n-L+1} F\left(L+\frac{i\alpha}{v};\, L-1-n;\, 2L;\, \frac{-4i\chi}{(\chi-i)^2}\right)\right] \tag{2.3}$$

with α the fine structure constant, m the electron rest mass, χ the ratio of the binding energy of Ps in the state n to the kinetic energy of the relative motion:

$$\chi = \frac{\alpha}{nv} \tag{2.4}$$

with:

$$0 \le \mathrm{arctg}\left(\frac{1}{\chi}\right) \le \frac{\pi}{2} \tag{2.5}$$

v is the velocity of the incoming particles, ω the energy of the outgoing photon and F(a,b,c,d) the hypergeometric function of four variables:

$$\omega = \frac{m\alpha^2}{4n^2} + \frac{mv^2}{4} \tag{2.6}$$

and:

$$F(a, b, c, d) = 1 + \frac{a.b}{1.c} d + \frac{a.(a+1).b.(b+1)}{1.2.} d^2 + \frac{a.(a+1)(a+2).b.(b+1).(b+2)}{c.(c+1) \quad 1.2.3 \quad .c.(c+1).(c+2)} d^3 \ldots \qquad (2.7)$$

Total radiative cross sections for the first ten quantum numbers are shown in Figure 1. At 100 eV, the damping factor between levels is well approximated by a $1/n^3$ law but it is not fit by any simple law for energies below 100 eV, although it approachs a power law behavior with index i = 1, for E = 0.01 eV (Figure 2). For low temperature plasma, radiative combination will thus populate appreciably higher quantum levels strengthening radio-wavelength transitions. Nevertheless, below 10^4 K, neutral atoms are important and charge exchange before thermalization will increase, even dominate, greatly reducing the total amount of Ps produced by the radiative combination process (Guessoum et al. 199 1). Moreover, it is not possible to neglect high azimuthal levels in typical astrophysical plasmas and crossings are observed between levels (Figure 3) and also sub-levels (Figure 4).

The Ps radiative combination reaction rates are calculated using:

$$R(n,L) = \int_0^\infty \sqrt{\frac{2}{\pi}}\, v^2 \left(\frac{\mu}{kT}\right)^{3/2} e^{-\left(\frac{\mu v^2}{2kT}\right)} . \sigma_{nL}(v) . v . dv \qquad (2.8)$$

where $R(n,L)$ is the radiative combination rate ($cm^3 . s^{-1}$) for the nL Ps state and μ the reduce mass of the Ps atom (Figure 5). We also represented the total radiative combination reaction rate R^{rc}, and the direct annihilation reaction rate R^{da}, computed from Gould (1989). The characteristic temperature ($R^{rc} = R^{da}$) calculated by Gould (1989) is $T_c = 6.8 \times 10^5$ K. If we take into account the ground state only, we find a lower

value of T_g = 3.7 x 10^5 K. Moreover, higher levels are always lower than the direct annihilation rate. We compared these results with the radiative combination rate in atomic hydrogen given in Table 2.1 in Osterbrock (1989) fern = 1 to 4 and n = 10. Different ratio $r(n,L) = R_{Ps}(n,L)/R_H(n,L)$ are presented for three temperatures in the range 5,000 K to 20,000" K in Figure 6. We see that this ratio is always lower than three but can decrease below one. The reason is that Ps combination reaction rates for high-L levels decrease faster than H-reaction rates at high temperature. The general trend is therefore a decrease of this ratio with increasing temperature.

3 POSITRONIUM CHARGE EXCHANGE CROSS SECTIONS

Charge exchange happens when a free positron and an electron in a bound state combine to form Ps. The major difference between charge exchange and radiative combination is the binding energy of the electron involved in the process which creates an energy threshold for the reaction. As previously noted by B urd yuzha et al. (1992) and Anantharamaiah et al. (1993), such thresholds are high enough to largely decrease thermal positronium formation by charge exchange in low temperature media (Table 3). Moreover, only low n levels will be populated. We therefore investigate here charge exchange processes in the n = 1 and 2 states for completeness only but these phenomena will be small in the regime studied here, Reaction rates are calculated using relation (2.8) where the lower integration limit is the energy threshold of the reaction and μ -m.

3. a POSITRON-ATOMIC HYDROGEN CHARGE EXCHANGE

Sperber et al. (1992) published the first measurements of the total charge exchange cross section with atomic hydrogen. No experiment results are yet available for the ground and first excited level. Moreover, theoretical calculations have focused on the low energy region below the Ps formation threshold and on the high energy region above around 50 eV (see Higgins and Burke 1993, for a recent review). In the energy band of interest here, theoretical results are scattered and not in good agreement with each other, particularly for the n = 2 level (e. g. Hewitt et al., 1990). Let us therefore point out that the results below are rough evaluations and both new experiments and theoretical work are strongly encouraged. We use here the result of Higgins and Burke (1993) based on a six-state approximation to model ground state charge exchange cross sections. For Ps(2s) and Ps(2p) we take the values from the Unitary Bom Approximation (UBA) with H(1s,2s,2p) + Ps(1s,2s,2p) basis (Hewitt et al.1990) because their Ps(2p) cross sections present only one maximum around 18 eV in good agreement with the one at 15 eV observed in the total charge exchange cross section measured by Sperber et al. (1992). Let us also point out that the charge exchange reaction rates have been incorrectly estimated in Wallyn et al. (1994 b). Using the above cross sections, the reaction rate at 5000 K is no more than ~ 3 times higher (and not more than one magnitude) than the value quoted in Bussard et al. (1979). Moreover, new H charge exchange cross section measurement by Weber et al. (1994) seems to indicate smaller cross sections than originally published by Sperber et al. (1992). Taking into account these new results, the charge exchange reaction rate for H is in good agreement with Bussard et al. (1979) computation. Therefore, we also plotted plotted our fit of the total cross sections, with lower values at low energy than previously published by Wallyn et al. (1994a). Reaction rates are calculated using relation (2.8) where the lower integration limit is the energy threshold of the reaction and $\mu \sim m$.

3. b POSITRON-HELIUM CHARGE EXCHANGE

Although there are several theoretical calculations of the charge exchange process between a free positron and an helium atom, no theory agrees well with experimental data (Charlton et al. 1983, Fornari et al. 1983, Diana et al. 1986, Fromme et al. 1986). Nevertheless, the high energy threshold of the first excited positron-He state (22.9 eV) which is far higher than the n = 2 energy threshold for H (11.9 eV) and the typical He abundance in most of the astrophysical environments make the He contribution to Ps formation one order of magnitude less than H. We used here the data from table 4 from Hewitt et al. (1992) for the 1s, 2s and 2p levels although these theoretical evaluations present maxima at slightly lower energy than in the experimental results and are significantly below them for energies above 50 eV. Our fit of the total cross section is taken from Chapuis et al. (1994) - (Figure 8).

3. c POSITRON-MOLECULAR HYDROGEN CHARGE EXCHANGE

Several groups measured formation of the positron-hydrogen molecule (Fornary et al. 1983, Diana et al. 1986, Griffith et al. 1984, Fromme et al. 1988) but to our knowledge, no theoretical calculations of the ground state and 2s and 2p capture cross sections are available below 50 eV (e. g. Biswas et al. 199 1a, b). Nevertheless, the Ps energy threshold of 8.6 eV in H_2 makes positronium state more difficult to form in low temperature media than in H and typical temperatures encountered in molecular clouds are far below this threshold.

4 CAPTURE-CASCADE-ANNIHILATION EQUATIONS FOR POSITRONIUM

4. a RADIATIVE TRANSITIONS

We consider here an optically-thin and low density medium where excited states of positronium are populated by radiative capture of the free thermal positrons by electrons and by cascade from all higher Ps states and depopulated by cascade to lower levels *and* annihilation from excited states. This set of assumptions is commonly called Case A and assumes that all line photons emitted escape. We do not investigate here the Case B which assumes that every Lyman-line photon is scattered many times and converted into lower-series photons that increased higher transition strengths (Baker and Menzel 1938, Osterbrock 1989) because positrons in low temperature astrophysical media are usually a very minority specy compared to electrons or atomic hydrogen and therefore, any Lyman-line photon has a very small probability at interacting again with a Ps atom. A detailed study is needed, taking into account the photon contribution of other species. Case A, might be also accurate enough for a wide range of density situations because Gould (1989) evaluated the critical density, where capture-cascade-annihilation process will diverge from a pure radiative transition, to the order of 10^{15} cm^{-3}.

We use three equations of statistical equilibrium (one for each target species, e-, H and He) which can be solved independently:

$$n_{e^+} n_e R^{RR}_{nL} + \sum_{n' = n+1}^{n' = +\infty} \sum_{L' = L \pm 1} (N^{RR}_{n'L'} A_{n'L', nL}) = (N^{RR}_{nL} A_{nL}) \qquad (4.1)$$

and:

$$n_{e^+} n_i R^{ce}_{21} = N(i)^{ce}_{21} A_{21} \qquad (4.2)$$

where i corresponds to one of the two species, H and He, n_{e+}, n_{e-} and n_i are the positron, electron and (H or He) densities respectively. R is a reaction rate and the superscripts ce and rc correspond to the charge exchange and radiative combination reactions respectively. $A_{n'L',nL}$ is the probability in s^{-1} of *direct* transition from the state n'L' to nL. A_{nL} is the total probability of direct transition to all lower levels *plus* the annihilation rate in the state nL and N is the number per unit volume of Ps atoms in the state nL. The difference between (4.1) and (4.2) is that we only consider two levels populations (ground and first excited states) for atoms because of their energy thresholds and thus only Lyct transitions are expected, without cascades from the upper levels.

As we assume that collisional transitions n'L' to nL are less rapid than radiative transitions alone, we use the "nL method" developed by Pengelly (1964) which is valid for very low densities ($N_{e-} < 10^4\ cm^{-3}$) and optically thin media in Balmer line transition. The populations of quantum levels for Ps radiative combination are given by (Seaton 1959):

$$N_{nL} = \frac{n_{e+}n_{e-}}{A_{nL}} \sum_{n'=n}^{n'=+\infty} \sum_{L'=0}^{L'=n'-1} R_{n'L'}\, C_{n'L',nL} \qquad (4.3)$$

This expression is simplified in our evaluation of the Lyα transition from charge exchange processes and reduced to:

$$N_{21} = \frac{n_{e+}n_i}{A_{21}} R_{21} \qquad (4.4)$$

where $C_{n'L',nL}$ is the probability for a Ps atom in the state n'L' to be followed by a radiative transition to nL via *all* possible cascade paths. The intensity corresponding *to* the transition n'L'-->nL for radiative combination, is therefore:

$$I_{n'n} = \sum_{L'=0}^{L'=n'-1} \sum_{L=L'\pm1} N_{n'L'} A_{n'L',nL} \tag{4.5}$$

and for charge exchange it reduces to:

$$I^{i}_{21} = N^{i}_{21} A_{21,10} \tag{4.6}$$

and the total intensity $I_{n'n}$ is then the sum of the three above processes:

$$I_{n'n} = \sum_{i=1}^{i=3} I^{i}_{n'n} \tag{4.7}$$

In order to calculate Ps combination line intensities we must then evaluate the three following probabilities: (A), the probability to produce a Ps atom in the quantum state nL, (B) the probability for a positronium atom in the state nL to be followed by a transition to n'L' via *all* possible cascade paths and (C), the probability for a Ps atom in the state n'L' to do a radiative transition *directly* to n"L". The first probability depends directly of the reaction rate of the interaction producing Ps (charge exchange or radiative combination) but the last two probabilities will be independent of the production mechanism.

The probability for a positron in the state n'L' to be followed by a *direct* radiative transition to nL, $P_{n'L',nL}$, is calculated by using the dipole approximation. This approximation has been justified by Nieminen (1967). The radiative coefficients $A_{n'L',nL}$, for a hydrogenic ion of charge Z = 1 are given by :

$$A_{n'L',nL} = 4\pi^2 \nu^3 \left(\frac{8\pi \alpha a_0^2}{3 c^2}\right) \frac{\max(L,L')}{(2L'+1)} |p(n'L',nL)|^2 \qquad (4.8)$$

where a_0 is the Bohr radius, ν the wove-number of the transition n'L'-->nL and p(n'L',nL) the dipole matrix element (e. g. Pengelly 1964, Blocklehurst 1971). When this expression is used by remplacing the electron mass by the reduced mass of the positronium system, μ = m/2, in the wave-number expression:

$$\frac{\nu}{c} = \frac{1}{2} R_\infty \left(\frac{1}{n^2} - \frac{1}{n'^2}\right) \qquad (4.9)$$

where R_∞ is the Rydberg constant:

$$R_\infty = \frac{2\pi^2 m e^4}{c h^3} \qquad (4.10)$$

and in the Bohr radius formula:

$$a_0 = \frac{\hbar^2}{m e^2} \qquad (4.11)$$

The dipole approximation coefficients $A_{n'L',nL}$ for positronium are therefore divided by a factor two:

$$A_{n'L',nL} = 1.3387 \times 10^{9} a_{n'L',nL} \tag{4.12}$$

where:

$$a_{n'L',nL} = \left(\frac{1}{n^2} - \frac{1}{n'^2}\right)^3 \frac{\max(L,L')}{(2L'+1)} |p(n'L',nL)|^2 \tag{4.13}$$

We use here an expression given by Gordon (1929) where the degeneracy of the levels is not taken into account and check our results with the values of $[p]^2$ for $n \leq 20$ published by Green et al. (1957):

$$|p(n'L-1,nL)|^2 = \left(\frac{(-1)^{n'-1}}{4(2L-1)!}\sqrt{\frac{(n+L)!(n'+L-1)!}{(n-L-1)!(n'-L)!}}\frac{(4nn')^{L+1}}{(n+n')^{n+n'}}\right.$$

$$\left. \times (n-n')^{n+n',-2L-2} \left[{}_2F_1\left(-n+L+1, -n'+L, 2L, \frac{-4nn'}{(n-n')^2}\right) - \left(\frac{n-n'}{n+n'}\right)^2 {}_2F_1\left(-n+L-1, -n'+L, 2L, \frac{-4nn'}{(n-n')^2}\right)\right]^2\right. \tag{4.14}$$

where the convention here is that if the value of L is larger than L', the total quantum number for this state is n - in the other case we swap (n,L) and (n',L'). We thus have:

$$P_{n'L',nL} = \frac{A_{n'L',nL}}{A_{n'L'}} \tag{4.15}$$

where:

$$A_{n'L'} = \sum_{n''=1}^{n''=n'-1} \sum_{L''=L'\pm 1} A_{n'L',n''L''} + A_{a(n,L)} \tag{4.16}$$

represents the summation over all the lower allowable quantum states (according to Laporte law) and $A_a(n,L)$ is the inverse of the annihilation time in the excited state nL:

$$A_a(nL) = \frac{1}{\lambda_{nL}} \tag{4.17}$$

with:

$$\lambda_{nL} = \lambda_0 n^3 \left(\frac{e^2}{hc}\right)^{-2L} \tag{4.18}$$

where λ_o is the lifetime in the ground state (McKlintock 1984). Let us also mention that annihilation is only possible from the nL=0 states. For para-positronium λ_o = 1.25 x 10^{-10} s and for ortho-positronium λ_o = 1.41 x 10^{-7}s. Thus, most of the para-Ps in the quantum state (n,()) will annihilate before they cascade or radiate. This effect will decrease low n transitions but will have little effect on high n levels as the l=0 states are less and less populated (Fig. 3 and Fig. *4).* For exemple, $P_{30,21}$ is equal to 1 without annihilation and slightly reduces to 0.92 for ortho-Ps but decreases to 0.01 for the para-Ps state (Table 4).

We also need the probability for a positron in the state n'L' to be followed by a radiative transition to nL via *all* possible cascade paths, $C_{n'L',nL}$. It is possible to calculate these coefficients using a loop given by (e. g. Pengelly 1964):

$$C_{nL,nL} = 1 \qquad (4.19)$$

and then:

$$C_{n'L',nL} = \sum_{n''=n}^{n''=n'-1} \sum_{L''=l\pm 1} P_{n'L',n''L''} \; C_{n''L'',nL} \qquad (4.20)$$

The intensity of a given transition n-->n' is computed taking into account the branching ratio between para (1/4) and ortho (3/4) states. We first computed line intensities for the first fourteen quantum states, taking into account cascades from upper levels until n_{max} = 20. In order to evaluate the influence of the cascade from all the other upper levels ($n_{max} = \infty$) to these lines, we fitted the increased of a given line intensity between to successive values of n_{max} by a power-law. The general trend is a decrease of its index with n_{max}. We thus extrapolated this trend taking into account the decrease of the index of the last two power-law fits. Higher Ps

line transitions (until n = 134) have also been extrapolated from the results for n < 15 with the same method (Figure 9). This values must be therefore considered as a crude lower estimate of the true result.

4. b FINE AND HYPERFINE TRANSITIONS

The excited states of a hydrogen atom possess fine structure whose transitions between the sub-levels give lines in the radio band (Kaplan and Pikelner 1970). This is also the case for Ps (Table 2). We calculated the transition probability for the fine transitions in which the principal quantum number does not change using (Kaplan and Pikelner 1970):

$$A^{Ps}_{nL,n(L\pm1)} = 4 \times A^{H}_{nL,n(L\pm1)} = \frac{12}{(me)^2}\left(\frac{h\nu}{c}\right)^3 \frac{\max(L,L\pm1)}{2L+1}\, n^2(n^2-L^2) \qquad (4.21)$$

The transition (2^3S_1-1^3S_1) is far more probable than the previous ones but the transition cannot be separated from the Ly_α line and will not be studied here. The hyperfine transition in the ground state of Ps (1^3S_1-1^1S_0) is deduced from the expression given for hydrogen transitions (e.g. Lang 1980):

$$A^{Ps}_{10} = 4 \times A^{H}_{10} \approx 4 \times \frac{\pi^2 e^2 h}{c^5 m^2} \nu^3_{10} \approx 4 \times 10^{-42} \nu^3_{10} \qquad (4.22)$$

The relative intensities are calculated using expressions given in §4 above. Thus the fine structure intensities (2^3S_1-2^3P_J) reduce to:

$$I^J_{20,21} = N^{ortho}_{20} A^J_{20,21} = \frac{R(2,0)}{A^{ortho}_a(2,0) + A^J_{20,21}} A^J_{20,21} \qquad (4.23)$$

and the hyperfine transition:

$$I_{10} = N^{ortho}_{10} A_{10} = \frac{R(1,0)}{A^{ortho}_a(1,0) + A_{10}} A_{10} \qquad (4.24)$$

We neglect in the evaluation of I_{10}, the transition (2^3S_1-1^3S_1) because its probability (of the order of 4 S-t, Kaplan and Pilkener 1970) is far lower than the direct annihilation probability on the level n=2, L=O (A= 88 x 10^4 s^{-1}) and thus cannot appreciably populate the ground state (see Figure 1 in Burdyuzha et al. 1992). We extrapolated the intensity to $n_{max} = \infty$ with the same method as described in §4a.

4. c POSITRONIUM LINE WIDTHS

As we assumed that the electrons and positrons are thermally distributed, the difference of their relative speed will be also described by a Maxwell-Boltzman distribution and we usually consider that the positronium lines from radiative recombination are thermally broadened. The line width is therefore given by (McClintock 1984):

$$\frac{\Delta\lambda}{\lambda} = 1.30 \times 10^{-3} \left(\frac{T}{10^4 K}\right)^{0.5} \qquad (4.25)$$

keV line from the annihilation of thermal positronium was first given by Cranell et al. (1976). To calculate it, one assumes that a positron of relative energy E interacts with an electron to produce a positronium atom and that its velocity in the direction of the observer is given by a distribution ranging between:

$$v = \pm \sqrt{\frac{E}{m}} \qquad (4.26)$$

The relative width of the annihilation line is therefore given by the Doppler contribution of the 511 keV photons. This is also the case for the de-excitation Ps line. More recently, Guessoum et al. (1991) have re-analyses with a Monte-Carlo simulation the annihilation width for the combination process: they find that the electron-positron system is not exactly thermally distributed at the temperature of the gas. Their result is valid at. least between 8000K and 10^6 K. These authors find that the annihilation line is narrower by 29% at 8000 K and up to 42% at 4.5 x 10^5 K. Using their result, we thus have the following formula for the Ps de-excitation line width from the combination process:

$$\left(\frac{\Delta\lambda}{\lambda}\right)_{Ps} \approx 7.8X\ 10^{-4} \left(\frac{T}{10^4 K}\right)^{0.44} \qquad (4.27)$$

The charge exchange cross sections for the ground and excited states of H and He are not very accurate and we use the relative line width results described in Bussard et al. (1979) for the total charge exchange cross section of H. Assuming the same behavior as in (4.27), we approximate the Ps-Lyα line width for both H and He using:

$$\left(\frac{\Delta\lambda}{\lambda}\right)_{Ps} \approx 3.2X\ 10^{-3}\left(\frac{T}{10^4K}\right)^{0.41} \qquad (4.28)$$

5 RESULTS

In Figure O, we compared values of Ps de-excitation lines at 2×10^4 K with those for Hydrogen (Case A) given in Table 5 in Pengelly (1964). Our absolute intensities ($cm^{-3}.s^{-1}$) are in good agreement whith those of Pengelly and show a general decrease of the ratio I_{ps}/I_H with increasing excited transitions. Moreover, Ps intensities can be lower or higher than the corresponding H transitions, depending of the series and the temperature (see also Figure 6).

The different positron annihilation rates are shown in Figure 11. In order to allow an easy access to these results, we give in Table 5, the total annihilation reactions rates, R^i, for each of the above processes, i and the ratio $I_{ps}(Ly_\alpha)/R^{rc}$ of the absolute intensities for each transition and for a given process if the relative amount of e-, H and H_2 species are known. The relative contribution of the para and ortho states to the formation of the Ps lines have been compared to the Ps intensity when the annihilation from excited states are neglected: this effect is always low for transitions from n = 2 and n = 3 and negligible for higher transitions.

Table 6 gives the absolute intensities of Ps de-excitation lines for radiative combination and the Lyman-α absolute intensities for the charge exchange process for different temperatures are presented in Table 7. Our evaluation of the fine and hyperfine transitions for both the radiative recombination and charge exchange processes are given in Tables 8, 9 and 10. These transitions are much weaker than the corresponding de-

excitation lines because their transition probability is low and also because the annihilation probability for the ground state (A_a - 7 x 10^6).

As an example and in order to give indications on the best observing window to detect Ps de-excitation lines from a cosmic point source, we represent in Figure 12 the expected Ps luminous fluxes L_λ in Jansky (1Jy = 10^{-23} erg. $cm^{-2}.s^{-1}.Hz^{-1}$) for different values of the absorption coefficients A_λ:

$$L_\lambda = \frac{f}{(2-\frac{3}{2}f)} r^\pi r^\lambda \frac{I_\lambda \times E_\lambda}{\Delta\nu \times 2.512^{A'}} \qquad (5.1)$$

where I_λ is the 511 keV flux (in ph. $cm^{-2}.s^{-1}$), E_λ is the energy of a photon for a given Ps transition (in ergs), $\Delta\nu$ the Ps line width, f the positronium fraction after thermalization, A, the optical extinction, r^π the number of Ps Lyα photons for each positronium atom and r^λ the ratio $I(Ps_{Ly\alpha})/I(Ps_\lambda)$. We assume here a point source producing a 511 keV flux of 10^{-3} ph. $cm^{-2}.s^{-1}$ in an annihilation medium at T = 10^4 K. Moreover the pairs are supposed thermal and the medium constituted *only* of ionized atoms. From Table 5 we have f = 8670 and r^π = 0.32. The relative intensities of the Ps de-excitation series, r^λ is found in Table 6. The Ps line widths used to evaluate the luminous flux are evaluated using relation (4.27) and Table 1. The absorption coefficients are calculated using the extinction law toward the Galactic Center given by Rieke and Lebofsky (1985) and valid from 1 to 13 μm and the one of Mathis (1990) for longer wavelengths.

From Figure 13, we see that the best observing Ps line depends strongly of the visual extinction. Below A_V -5, the most intense Ps line is PsHα in the near-IR. For A_v - 10 to -25, we have PsPα and for A_v -50, PsBrα in the mid-IR. Moreover, the millimeter and centimeter Ps transitions are in any case much weaker than lower n transitions. For ground telescopes, the best observing window is therefore in the IR band.

ACKNOWLEDGEMENT

The authors thank Vladimir Burdyuzha, Richard Drachman and Vladimir Kauts for very helpful comments. The research described in this paper was carried out by the Jet Propulsion Laboratory, California institute of Technology, under contract to the National Aeronautics and Space Administration,

REFERENCES:

Anantharamaiah, K. R., Radhakrishnan, V., Morris, D., Vivekanand, M., Dowries, D., and Shukre, C. S. 1989, in *Galactic Center,* ed. M. Morris (Dordrecht: Kluwer), p. 607.

Anantharamaiah, K. R., Dwarakanath, K. S., Morris, D., Goss, W. M., & Radhakrishnan, V. 1993, Ap. J., 410, 110.

Baker, J. G., and Menzel, D. H. 1938, Ap. J., 88, 52.

Biswas, P. K., Mukherjee, T., and Ghosh, A. S. 1991, J. Phys. B: At. Mol. Opt. Phys., 24, 2601.

Biswas, P. K., Madhumita Basu, Ghosh, A. S., and Darewych, J. W. 1991, J. Phys. B: At. Mol. Opt. Phys.,24, 3507.

Brocklehurst, M. 1971, M. N. R. A. S., 153, 471.

Burdyuzha, V. V., Chechetkin, V. M., Mickevich, A. S., Shantarovich, V. P., & Yudin, N. P. 1987, *ESO workshop on the SN 1987A,* ed. Danziger, p 113.

Burdyuzha, V. V., Kauts, V. L., and Yudin, N. P. 1992, A. & A., 255, 459.

Burdyuzha, V. V., and Kauts, V. L. 1994, Ap. J. Supp., 92, 549.

Bussard, R. W., Ramaty, R., and Drachman, R. J. 1979, 228, 928.

Canter, K. F., Mills, A. P. Jr., and Berko, S. 1975, Phys. Rev. Letters, 34, 177.

Chapuis, C., Wallyn, P., and Durouchoux, Ph. 1994, Ap.J. Supp., 92, 545.

Charlton, M., Clark, G., Griffith, T. C., and Heyland, G. R. 1983, J. Phys. B: At. Mol. Phys. 16, L465.

Chu, S., and Mills, A. P. 1982, Phys. Rev. Lett. 48, 1333.

Cranell, C. J., Joyce, G., Ramaty, R., and Wemtz, C. 1976, Ap. J., 210, 582.

Diana, L. M., Coleman, P. G., Brooks, D. L., Pendleton, P. K., and Norman, D. M. 1986, Phys. Rev. Lett. 34, 2731.

Deutsch, M., 1951, Phys. Rev. 82, 455.

Fornari, L. S., Diana, L. M., and Coleman, P, G. 1983, Phys. Rev. Lett. 51, 2276.

Fromme, D., Kruse, G., Raith, W., and Sinapius, G. 1986, Phys. Rev. Lett. 57, 3031.

Fromme, D., Druse, G., Raith, W., and Sinapius, G. 1988, J. Phys. B: At. Mol. Phys. 16, L465.

Gould, R. J. 1989, Ap. J., 344, 232.

Gordon, W. 1929, Ann. der. Phys., (5), 2, 1031.

Green, L. C., Rush, P. P., and Chandler, C. D. 1957, Ap.J. Sup., 3, 37.

Griffith, T. C. 1984, in *Positron* Scattering *in Gases*, eds. Humberston and McDowell, (New York, Plenum), p 53.

Guessoum, N., Ramaty, R., and Lingenfelter, R. E., 1991, Ap.J., 378, 170

Hagena, D., Ley, R., Weil, D., Werth, G., Arnold, W., and Schneider, H. 1993, Phys. Rev. Letters, 71, 2887.

Hewitt, R. N., Noble, C. J., and Bransden, B. H. 1990, J. Phys. B: At. Mol. Opt. Phys., 23, 4185.

Hewitt, R. N., Noble, C. J., and Bransden, B. H. 1992, J. Phys. B: At. Mol. Opt. Phys., 25, 557.

Higgins, K., and Burke, P. G. 1993, J. Phys. B: At. Mol. Opt. Phys., 26, 4269.

Joyce, R. R., 1992, in *Astronomical CCD Observing and Reduction Techniques,* ASP Conf. Series, ed. Howell, Vol. 23, p 258.

Kaplan, S. A., and Pikelner, S. B. 1970, in *The interstellar Medium*, Harvard University Press.

Lang, K. R. 1980, *Astrophysical Formulae*, Springer-Verlag.

Mathis, J. S. 1990, Annu. Rev. Astron. Astrophys., 28, 37.

McClintock, J. E. 1984, Ap. J., 282, 291.

Mills, A. P., Jr., Berko, S., and Canter, K. F. 1975, Phys. Rev. Lett. 34, 1541.

Mohorovicic, S. 1934, Astr. Nach., 253, 94.

Nicminen, I. 1967, Ark. f. Fys. 35, 1.

Osterbrock, D. E. 1989, *Astrophysics of Gaseous Nebulae and Active Galactic Nuclei,*

University Science Books.

Pengelly, R. M. 1964, M. N. R. A. S., 127, 165.

Rieke, G. H., and Lebofsky, M. J., 1985, Ap.J., 288, 618.

Seaton, M. J. 1959, M. N. R. A. S., 119, 7.

Sperber, W., Becker, D., Lynn, K. G., Raith, W., Schwab, A., Sinapius, G., Spicher, G., and Weber, M. 1992, Phys. Rev. Lett., 68, 3690.

Stobbe, M. 1930, Ann. der Phys., (5), 7, 661.

Wallyn, P., Durouchoux, Ph., Chapuis, C., and Leventhal, M. 1994a, Ap. J., 422, 610.

Wallyn, P., Chapuis, C., and Durouchoux, Ph. 1994b, Ap.JS., 92, 551.

Weber, M., Hofmann, A., Raith, W., Sperber, W., Jacobsen, F., and Lynn, K. G. 1994, Hyperfine Interactions, 89, 221.

n	n'	transition	λ	band
2	1	Ly_α	2430 Å	UV
3	1	Ly_β	2051	
3	2	H_α	1.312 μm	near-IR
4	2	H_β	0.972	visible
4	3	Pa	3.749	near-IR
5	3	P_β	2.563	
5	4	Bra	8.100	mid-IR
6	4	Br_β	5.249	
6	5	Pf_α	14.91	mid-IR
7	5	Pf_β	9.302	
7	6	Hu_α	24.73	
8	6	Hu_β	15.00	
8	7	$Ps7_\alpha$	38.10	far-IR
9	7	$Ps7_\beta$	22.61	near-IR
9	8	$Ps8_\alpha$	55.57	far-IR
10	8	$Ps8_\beta$	32.40	
10	9	PS9a	77.70	
11	10	PS10α	105.0	
12	11	Ps11α	138.1	
13	12	Ps12α	177.4	
14	13	Ps13α	223.6	
15	14	PS14a	277.2	
16	15	Ps15α	338.6	
17	16	Ps16α	408.6	sub-mm
18	17	Ps17α	487.6	
19	18	Ps18α	576.1	
33	32	Ps32α	3.127 mm	mm
88	87	Ps87α	6.104 cm	cm
90	89	Ps89α	6.533	
130	129	Ps129α	19.79	
134	133	Ps133α	21.68	

TABLE 1: principal Ps transitions studied in this paper. Ly=Lyman, H=Balmer, P=Paschen, Br=Brackett, Pf=Pfund and Hu=Humphreys. The definitions of the different wavelength demarcation are based on modem detector capabilities and taken from Joyce (1992).

transition	λ	band	A (s^{-1})
fine-structure transitions (n= 1 and n=2)			
2^3S_1-1^3S_1	2430 Å	UV	2.06 X 10^{-5}
2^3S_1-2^3P_0	1.620 cm	c m	6.86 x lo-f'
2^3S_1-2^3P_1	2.304		2.39 X 10^{-5}
2^3S_1-2^3P_2	3.476		6.95 x 10^{-6}
hyper-fine transition (n=1)			
1^3S_1-1^1S_0	1.474mm	mm	3.37x 10^{-8}

TABLE 2: Ps fine and hyper-fine transitions observed in laboratory. A is the transition probability calculated using (4.22) and (4.23). For the transition 2^3S_1-*13S* $_1$, *we* use 0.25 x $A(H)_{2s1s}$ from Kaplan and Pikelner (1970).

reaction	E. (eV)
$e^+ + H(n=1) \rightarrow Ps(n=1) + H^+$	6.8
$e^+ + H(n=1) \rightarrow Ps(n=2) + H^+$	11.9
$e^+ + He(n=1) \rightarrow Ps(n=1) + He^+$	17.8
$e^+ + He(n=1) \rightarrow Ps(n=1) + He^+$	22.9
$e^+ + H_2(n=1) \rightarrow Ps(n=1) + 2H$	8.6
$e^+ + H_2(n=1) \rightarrow Ps(n=1) + 2H$	13.7

TABLE 3: first two energy thresholds for positron charge exchange with H, He and H_2.

nL	n'L'	P	P_{ortho}	P_{para}
(3,0)	(2,1)	1	0.923	0.011
(4,0)	*(2,1)*	*0.584*	*0.556*	0.010
(4>0)	(3,1)	0.416	0.396	0.007
(4,1)	(1,0)	0.839	0.839	0.839

TABLE 4: P: probability for an hydrogen atom to cascade directly from a level nL to the level n'L' during the recombination process; P_{ortho}: probability for a Ps atom to cascade directly from a level nL to the level n'L' in the ortho-Ps state; P_{para}: same probability for the para-Ps state.

	Temperature (K)					
	1000	5000	10^4	2 x 10'$	10^5	10^6
R^{da}	7.03(-13)	*2.40(-13)*	*1.59(-13)*	*1.07(-13)*	*4.71(-14)*	*1.78(-14)*
R^{rr}	*5.03(-13)*	*1.61(-12)*	*9.83(-13)*	*5.73(-13)*	*1.44(-13)*	*1.28(-14)*
R^{H}		4.6 (-15)	1.9 (-11)	1.4 (-09)		
R^{He}			5.7 (-18)	2.6 (-13)		
r^{rr}	0.45	0.37	0.32	0.28	0.18	0.09
r^{H}		2.4 (-4)	1.1 (-3)	1.8 (-2)		
r^{He}			1.8 (-3)	2.5 (-2)		

TABLE 5: total reaction rates, R, (per target density) in $cm^3.s^{-1}$ and ratio r of the absolute Lyman alpha intensity to the corresponding total reaction rate. da: direct annihilation, rr: radiative combination. The values in parenthesis represent the power of 10.

radiative combination

		Temperature (K)					
n	n'	1000	5000	10^4	2×10^4	10^5	10^6
2	1	2.27(-12)	6.05(-13)	3.18(-13)	1.58(-13)	2.54(-14)	1.11(-15)
3	1	*3.65(-13)*	1.20(-13)	6.86(-14)	3.70(-14)	6.41(-15)	2.91(-16)
3	2	1.25(-12)	2.76(-13)	1.33(-13)	6.11(-14)	9.30(-15)	4.95(-16)
4	2	2.89(-13)	7.66(-13)	3.90(-14)	1.93(-14)	2.87(-15)	1.39(-16)
4	3	6.69(-13)	1.18(-13)	5.09(-14)	2.05(-14)	2.31(-15)	8.97(-17)
5	3	1.98(-13)	4.18(-13)	1.91(-14)	8.53(-15)	9.93(-16)	3.77(-17)
5	4	3.89(-13)	5.92(-14)	2.37(-14)	8.80(-14)	8.07(-16)	2.52(-17)
6	4	1.37(-13)	2.43(-14)	1.03(-14)	4.29(-15)	4.11(-16)	1.28(-17)
6	5	2.37(-13)	3.23(-14)	1.23(-14)	4.29(-15)	3.36(-16)	9.15(-18)
7	5	9.51(-14)	2.43(-14)	5.95(-15)	2.36(-15)	1.92(-16)	5.27(-18)
7	6	1.50(-13)	1.88(-14)	6.85(-15)	2.27(-15)	1.57(-16)	3.96(-18)
8	6	6.70(-14)	1.49(-14)	3.63(-15)	1.37(-15)	9.83(-17)	2.46(-18)
8	7	9.89(-14)	1.15(-14)	3.93(-15)	1.29(-15)	8.04(-17)	1.93(-18)
9	7	4.80(-14)	9.45(-15)	2.31(-15)	8.40(-16)	5.36(-17)	1.27(-18)
9	8	6.74(-14)	7.36(-15)	2.51(-15)	7.68(-16)	4.40(-17)	1.03(-18)
10	8	3.50(-14)	6.24(-15)	1.52(-15)	5.33(-16)	3.09(-17)	7.08(-19)
10	9	4.76(-14)	4.90(-15)	1.62(-15)	4.78(-16)	2.55(-17)	5.92(-19)
11	10	3.38(-14)	3.40(-15)	1.03(-15)	3.09(-16)	1.56(-17)	3.60(-19)
12	11	2.57(-14)	2.45(-15)	7.55(-16)	2.07(-16)	9.89(-18)	2.29(-19)
13	12	2.11(-14)	1.86(-15)	5.47(-16)	1.44(-16)	6.51(-18)	1.51(-19)
14	13	1.7 (-14)	1.4 (-15)	4.1 (-16)	1.0 (-16)	4.4 (-18)	1.0 (-19)
15	14	1.4 (-14)	1.1 (-15)	3.1 (-16)	7.5 (-17)	3.1 (-18)	7.2 (-20)
16	15	1.3 (-14)	9.1 (-16)	2.4 (-16)	5.6 (-17)	2.2 (-18)	5.2 (-20)
17	16	1.1 (-14)	7.4 (-16)	1.9 (-16)	4.2 (-17)	1.6 (-18)	3.8 (-20)
18	17	9.4 (-15)	6.1 (-16)	1.5 (-16)	3.2 (-17)	1.2 (-18)	2.8 (-20)
19	18	8.2 (-15)	5.0 (-16)	1.2 (-16)	2.5 (-17)	9.0 (-19)	2.1 (-20)
33	32	2 (-15)	7 (-17)	1 (-17)	2 (-18)	5 (-20)	1 (-21)
88	87	2 (-16)	2 (-18)	3 (-19)	2 (-20)	3 (-22)	8 (-24)
90	89	2 (-16)	2 (-18)	2 (-19)	2 (-20)	3 (-22)	7 (-24)
130	129	7 (-17)	6 (-19)	5 (-20)	4 (-21)	4 (-23)	1 (-24)
134	133	7 (-17)	6 (-19)	5 (-20)	3 (-21)	3 (-23)	9 (-25)

TABLE 6: absolute intensities, I_{Ps}, of Ps de-excitation lines ($cm^{-3}.s^{-1}$) for the radiative combination process for a range of temperatures (the values in parenthesis represent the power of lo).

charge exchange

		Temperature (K)		
n	n'	5000	10^4	2 x 10'$
hydrogen:				
2	1	1.1(-18)	2.1 (-14)	2.5 (-11)
helium:				
2	1		1.0 *(-20)*	*6.6 (-15)*

TABLE 7: absolute intensities, $I_{Ly\alpha}$ of Ps de-excitation lines ($cm^{-3}.s^{-1}$) for charge exchange processes with H and He and for a range of temperatures (the values in parenthesis represent the power of 1O).

radiative combination

	Temperature (K)					
	1000	5000	10^4	' 2 x 10^4	10^5	10^6
fine transition (n= 1 and n=2):						
2^3S_1-2^3P_0	2.4(-23)	9.7(-24)	6.4(-24)	4.0(-24)	1.1(-2,4)	1.0(-25)
2^3S_1-2^3P_1	8.3(-24)	3.4(-24)	2.2(-24)	1.4(-24)	4.0(-25)	3.6(-26)
2^3S_1-2^3P_2	2.4(-24)	9.8(-25)	6.4(-25)	4.1(-25)	1.2(-25)	1.0(-26)
hyper-fine transition (n=1):						
1^3S_1-1^1S_0	*2.1(-26)*	*7.0(-27)*	*4.2(-27)*	*2.5(-27)*	*6.2(-28)*	*5.2(-29)*

TABLE 8: absolute intensities of Ps fine and hyperfine lines ($cm^{-3}.s^{-1}$) from the radiative recombination process for a range of temperatures (the values in parenthesis represent the power of lo).

Table 9: charge exchange with hydrogen

	Temperature (K)		
	5000	10^4	2×10^4
fine transition (n=1 and n=2):			
$23s_1$-2^3P_0	7. (-31)	7. (-26)	1. (-22)
2^3S_1-2^3P_1	3. (-31)	3. (-26)	4. (-23)
2^3S_1-2^3P_2	8. (-32)	7. (-27)	1. (-23)
hyper-fine transition (n=1):			
1^3S_1-1^1S_0	2. (-29)	*9. (-26)*	*7. (-24)*

Table 10: charge exchange with helium

	Temperature (K)	
	10^4	2 X 1 0 4
fine transition (n= 1 and n=2):		
2^3S_1-2^3P_0	8. (-33)	*3. (-25)*
2^3S_1-2^3P_1	3. (-33)	*9. (-26)*
2^3S_1-2^3P_2	8. (-34)	*3. (-26)*
hyper-fine transition (n=1):		
1^3S_1-1^1S_0	3. (-32)	*1. (-27)*

TABLE 9 **and 10**: absolute intensities of Ps fine and hyperfine lines ($cm^{-3}.s^{-1}$) from charge exchange reaction with hydrogen atoms (8a) and helium atoms (8 b), for a range of temperatures (the values in parenthesis represent the power of 10).

FIGURE CAPTIONS

FIGURE 1: Total Ps radiative combination cross section σ^n, for principal quantum state n, from n = 1 to 10 and also for n = 20 versus the relative kinetic energy of the incoming particles, taken from Table 5-20 in Nieminen (1967).

$$\sigma^n = \sum_{L=0}^{L=n-1} \sigma_{nL}$$

FIGURE 2: Ratio of the total Ps radiative combination cross section, σ^n to σ^1 for a given relative electron-positron kinetic energy E and for principal quantum number taken from n =1 to 20. The dots represent the values taken from Table 5-20 in Nieminen (1967) and the lines are the best fit power-laws with index i.

FIGURE 3: Ps radiative combination cross sections $\sigma(n,L)$, for the first three n levels versus the relative kinetic energy E. Crossings between n-levels are shown.

FIGURE 4: Ps radiative combination cross sections for n = 10 versus the relative kinetic energy E. Crossings between sub-levels are shown.

FIGURE 5: Ps radiative combination reaction rates, R(n,L) for n = 1 to n = 3, versus the temperature. The dashed and dot curves represent the direct annihilation, R^{da}, and total recombination rates, R^{rc}, of positrons with free electrons computed from Gould (1989). T_c and T_g are the temperatures where $R^{da} = R^{rc}$ and R^{da} = R(1 ,0) respectively.

FIGURE 6: ratio r(n,L) between the Ps radiative combination reaction rate, $R_{Ps}(n,L)$ and the hydrogen radiative recombination rate $R_{H}(n,L)$ for the n = 4 sub-levels and n = 10, L = O and for three temperatures: 5 x 10^3, 10^4 and 2 x 10^4 K. The curves are not fits on the data but link the ratios of given n and L.

FIGURE *7:* positron-hydrogen charge exchange cross sections. The cross sections for the formation of Ps to the ground state 1s = σ(1, O) are from Higgins and Burke (1993). The 2s = σ(2,0) and 2p = 0(2,1) cross sections are from Hewitt et al. (1990). The sum of the above cross sections are also represented (σ^1 -t- σ^2). The dashed curve is a fit of the total cross section from Wallyn et al. (1994) with lower values at low energies. The measured values are taken from Sperber et al. (1992).

FIGURE 8: positron-helium charge exchange cross sections. The cross sections for the formation of Ps to the ground state 1s and for the 2s and 2p states are from Higgins and Burke (1993). The sum of the above cross sections ($\sigma^1 + \sigma^2$) is compared to a fit of the total cross section from Chapuis et al. (1994, dashed curve). The experimental values are taken from Fornari et al. (1983) and Fromme et al, (1986).

FIGURE 9: Ps line flux (n--> n-l) for different values of n up to n = 14. The dashed curve is the flux evaluation taken into account cascades from the 20 first levels. The continued curve is the extrapolated flux for an infinite number of cascades up to n = 134.

FIGURE 10: comparison of the Balmer and Paschen I_{Ps}/I_{H} ratios for the combination process. The data for hydrogen are taken from Pengelly (1964).

FIGURE 11: positron charge exchange reaction rates for the first three sub-levels (1s, 2s and 2p) of H and He. The dotted lines R^{H} and R^{He} are the fitted total reaction rates.

FIGURE 12: luminous Ps fluxes (in Jy) expected from a point source which emits 10^{-3} $ph.cm^{-2}.s^{-1}$ at 511 keV (see §5 for details). The different transitions n--> n' are quoted in Table 1.

FIGURE 1

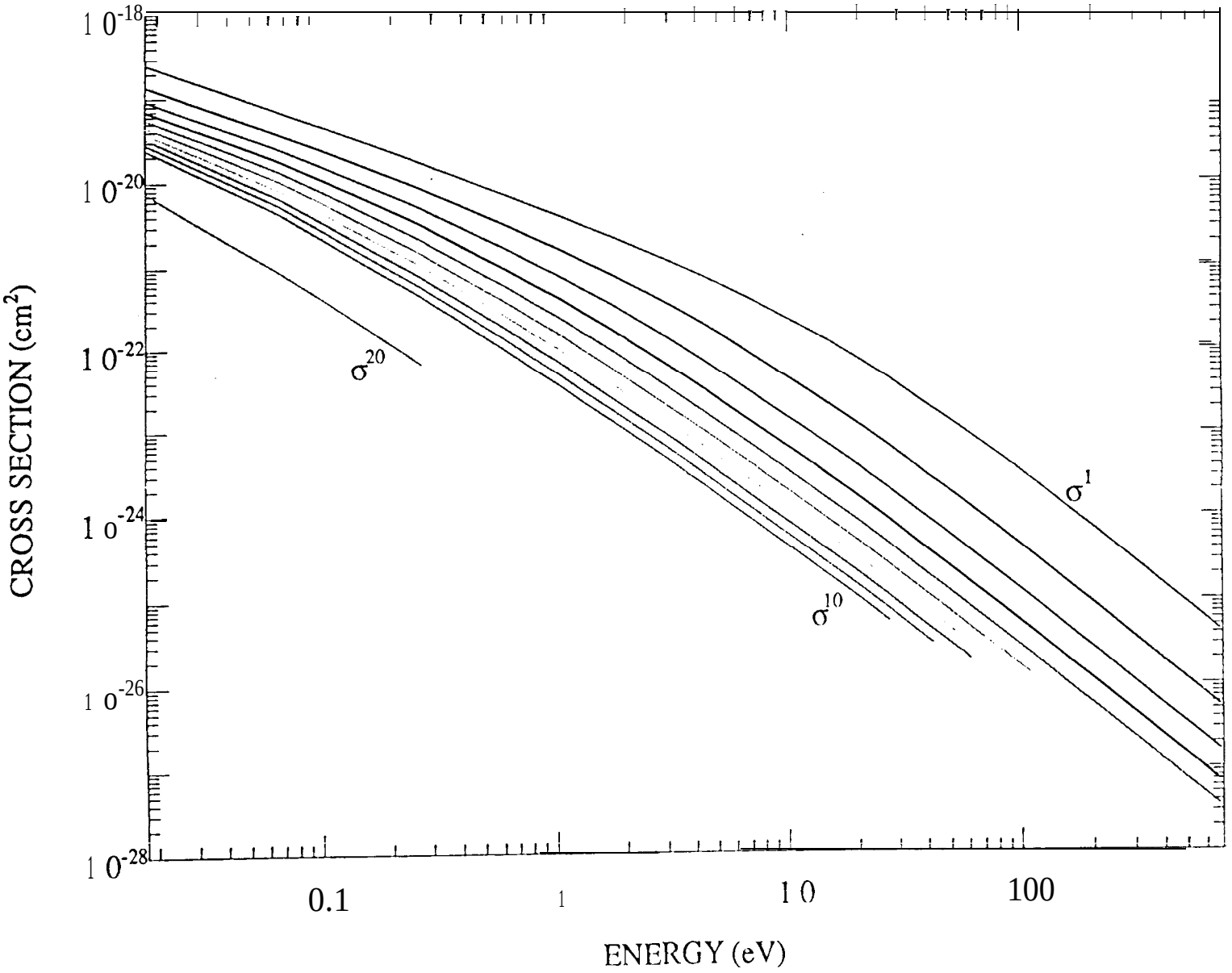
1 0^-18
1 0^-20
1 0^-22
1 0^-24
1 0^-26
1 0^-28
CROSS SECTION (cm^2)
σ^20
σ^10
σ^1
0.1
1
1 0
100
ENERGY (eV)

FIGURE 2

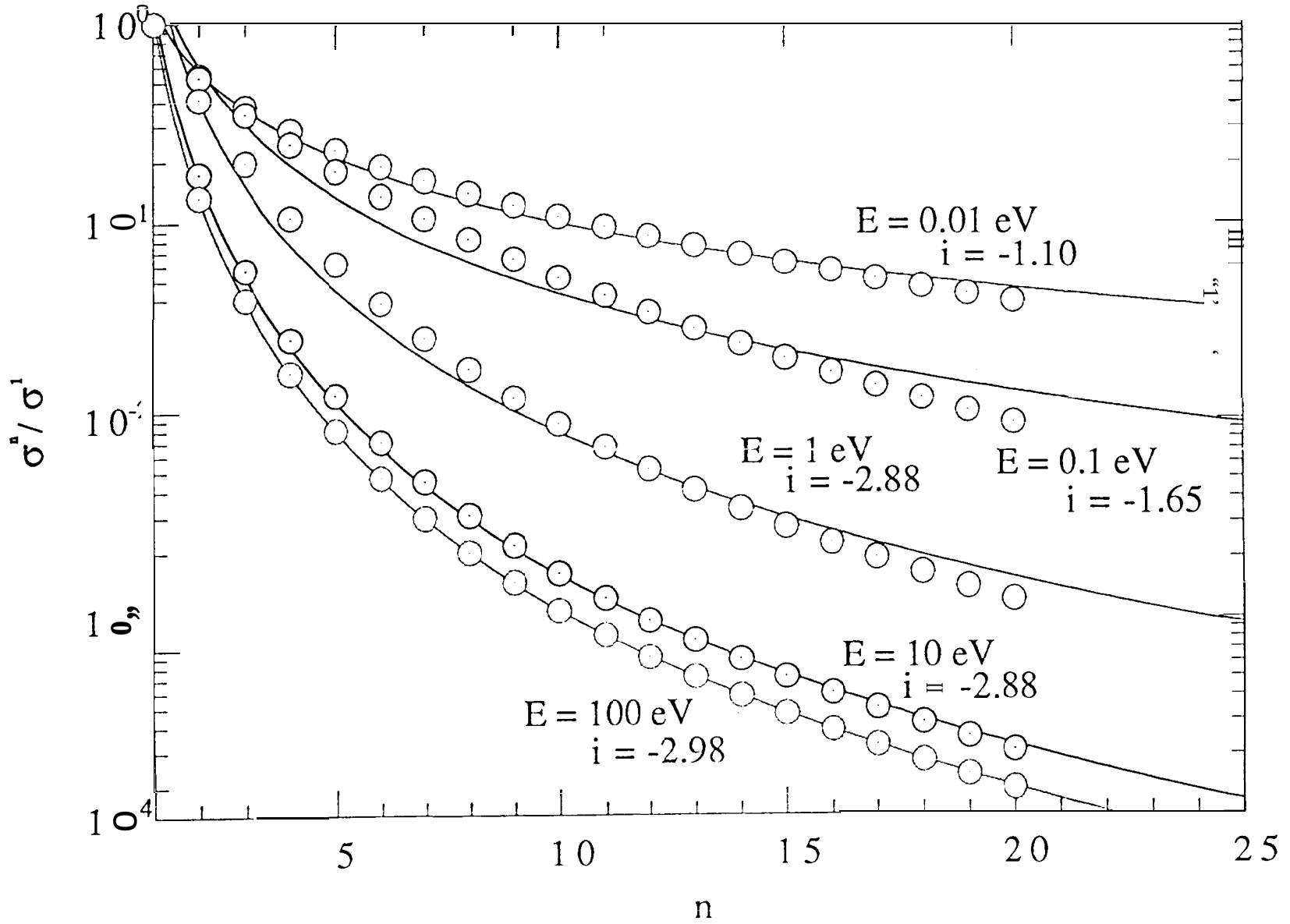
E = 0.01 eV
i = -1.10
E = 1 eV
i = -2.88
E = 0.1 eV
i = -1.65
E = 10 eV
i = -2.88
E = 100 eV
i = -2.98
σ^n / σ^1
n

FIGURE 3

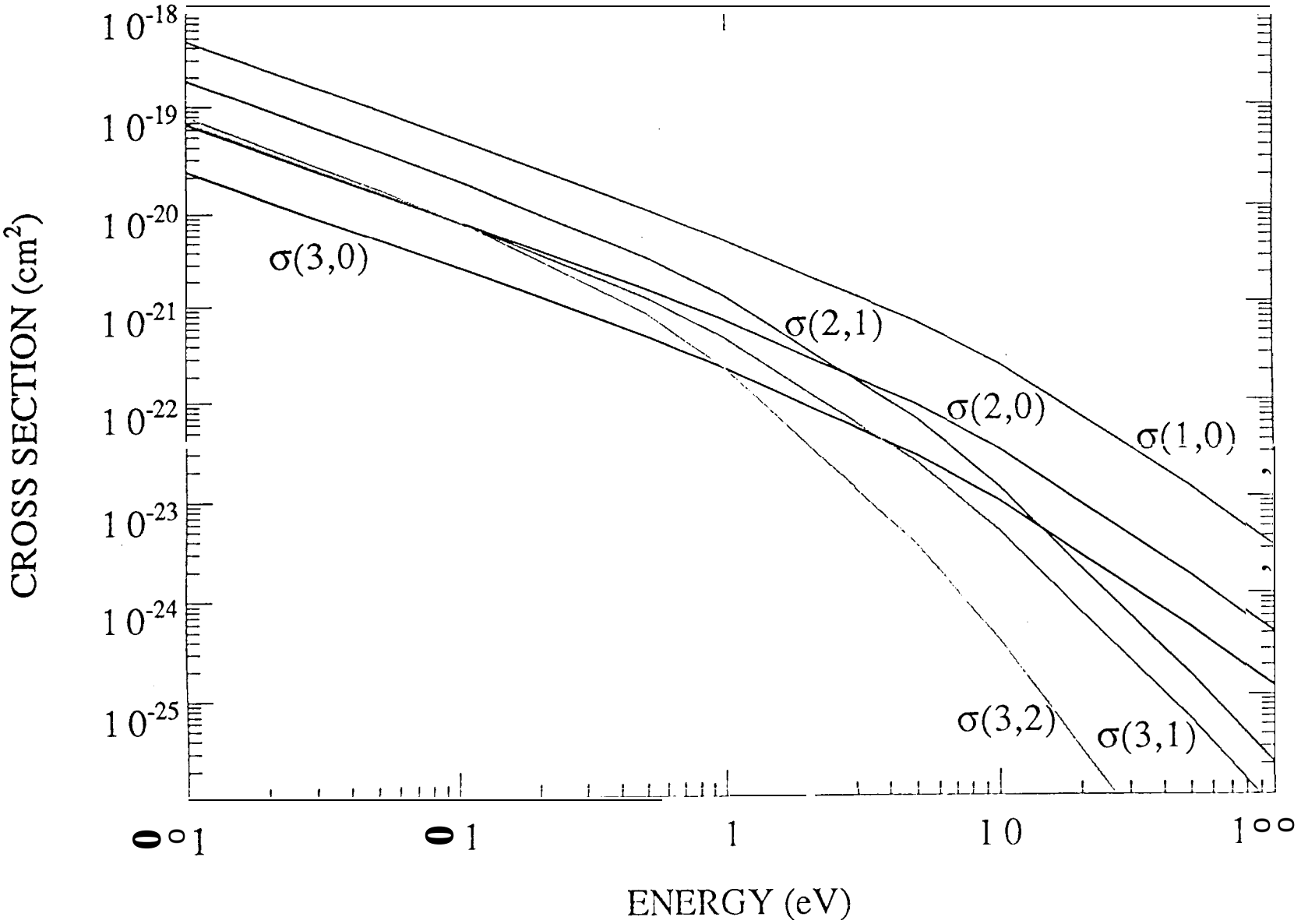
CROSS SECTION (cm²)
1 0-18
1 0-19
1 0-20
1 0-21
1 0-22
1 0-23
1 0-24
1 0-25
σ(3,0)
σ(2,1)
σ(2,0)
σ(1,0)
σ(3,2)
σ(3,1)
0 0 1
0 1
1
1 0
1 0 0
ENERGY (eV)

FIGURE 4

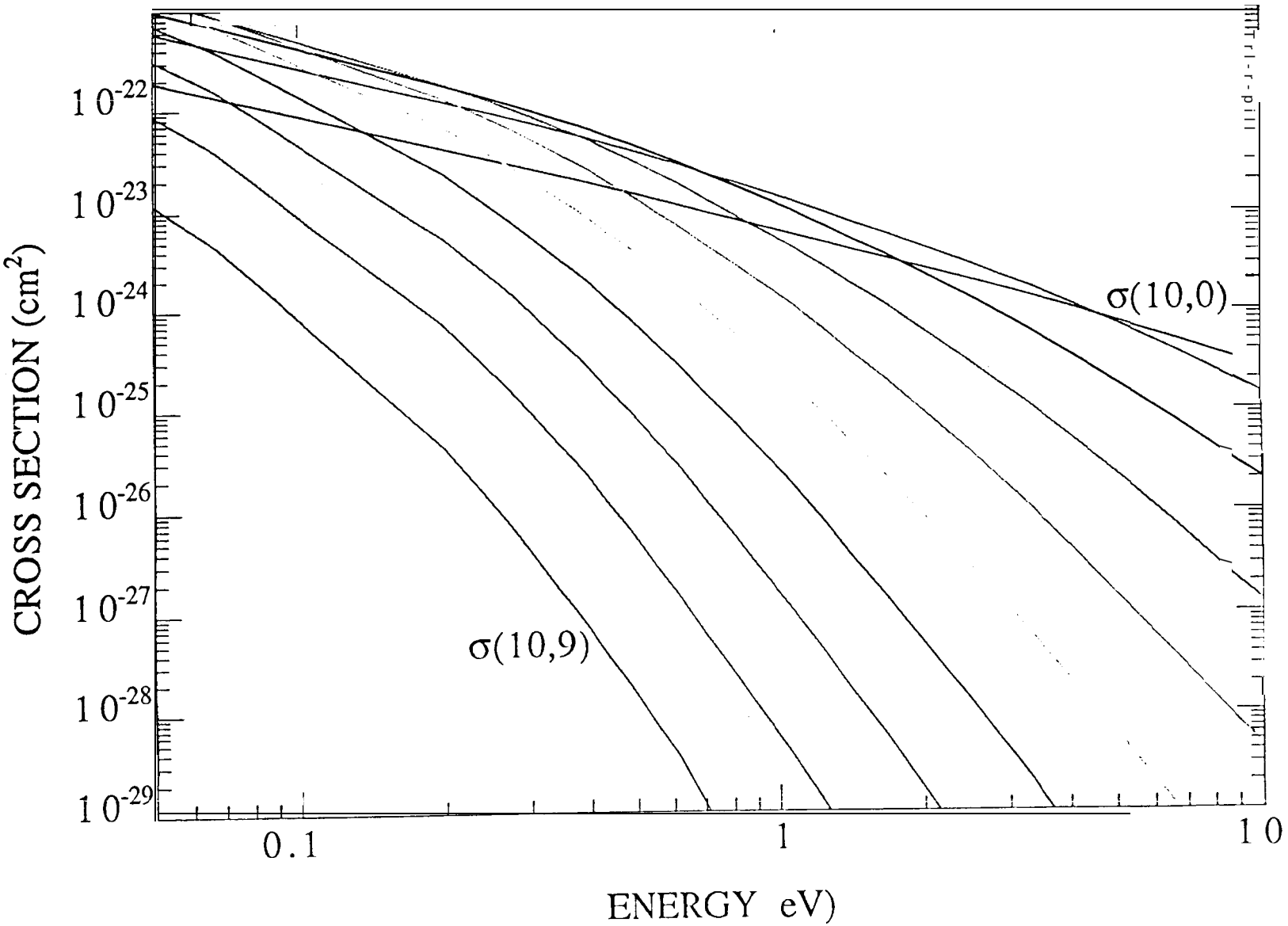
CROSS SECTION (cm^2)
10^{-22}
10^{-23}
10^{-24}
10^{-25}
10^{-26}
10^{-27}
10^{-28}
10^{-29}
σ(10,0)
σ(10,9)
0.1
1
10
ENERGY eV)

FIGURE 5

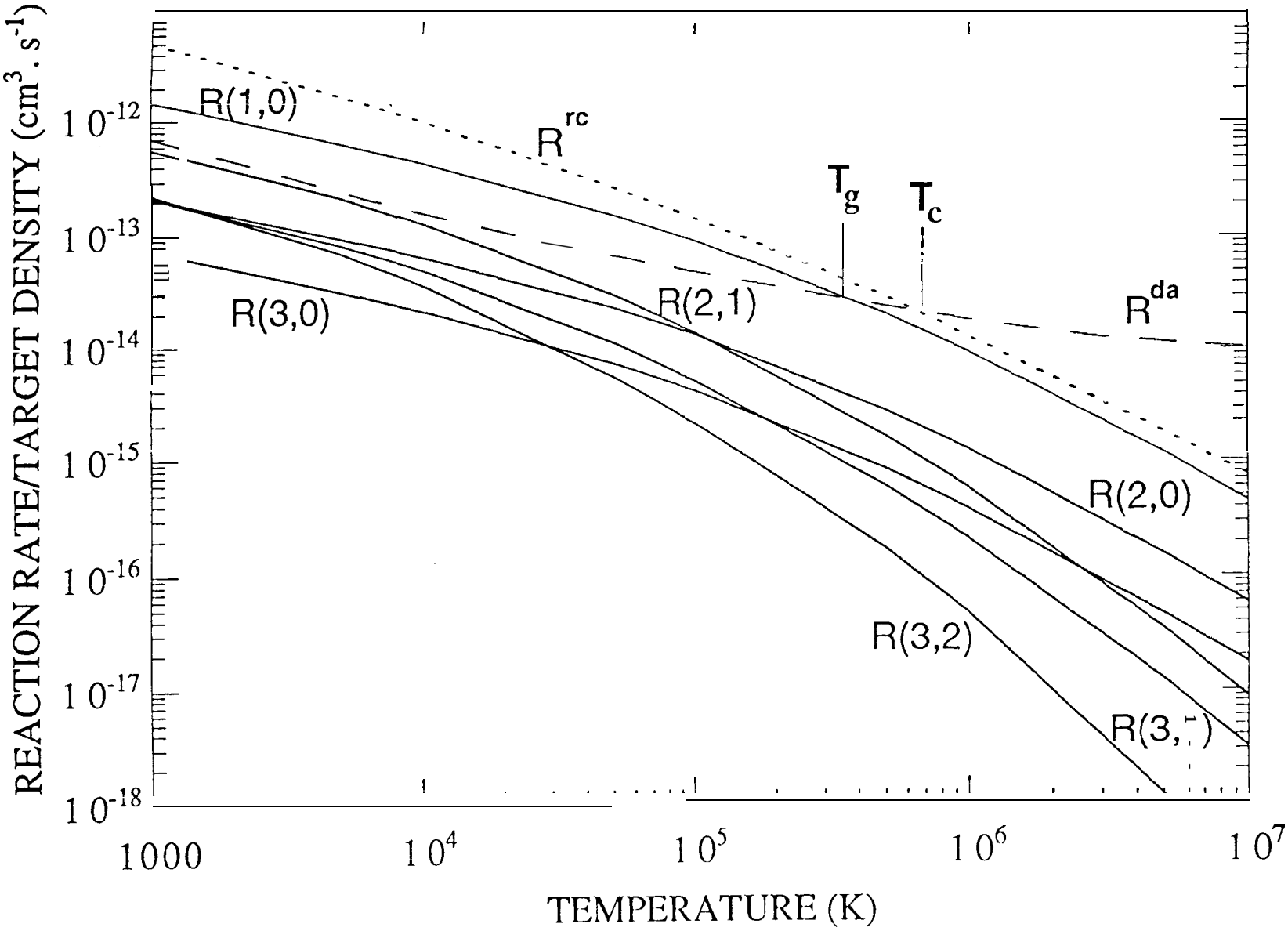
REACTION RATE/TARGET DENSITY (cm^3.s^{-1})
10^{-12}
10^{-13}
10^{-14}
10^{-15}
10^{-16}
10^{-17}
10^{-18}
R(1,0)
R^{rc}
T_g
T_c
R(2,1)
R^{da}
R(3,0)
R(2,0)
R(3,2)
R(3,
1000
10^4
10^5
10^6
10^7
TEMPERATURE (K)

FIGURE 6

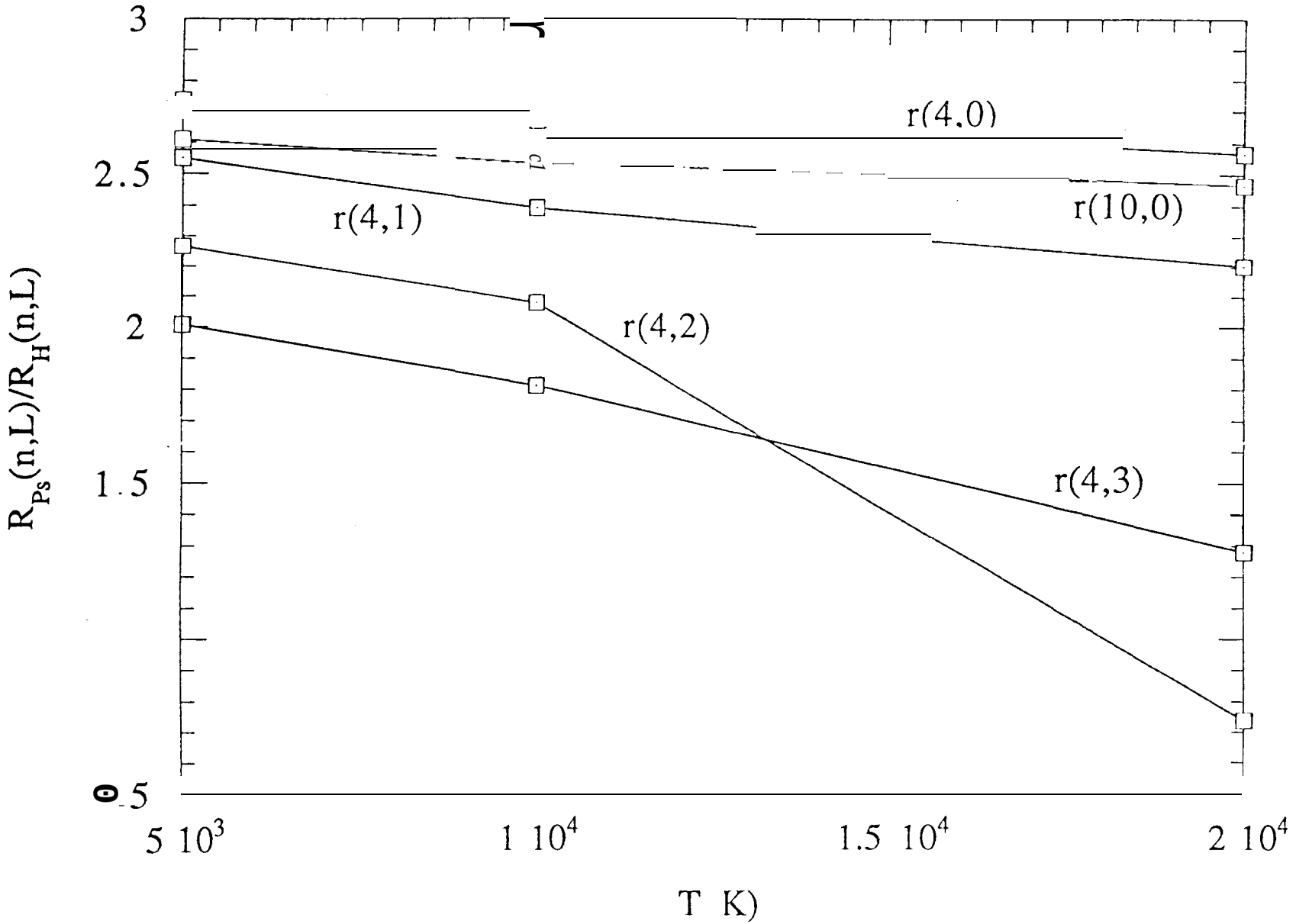
3
2.5
2
1.5
0.5
$R_{Ps}(n,L)/R_H(n,L)$
r(4,0)
r(4,1)
r(10,0)
r(4,2)
r(4,3)
5 10^3
1 10^4
1.5 10^4
2 10^4
T K)

FIGURE 7

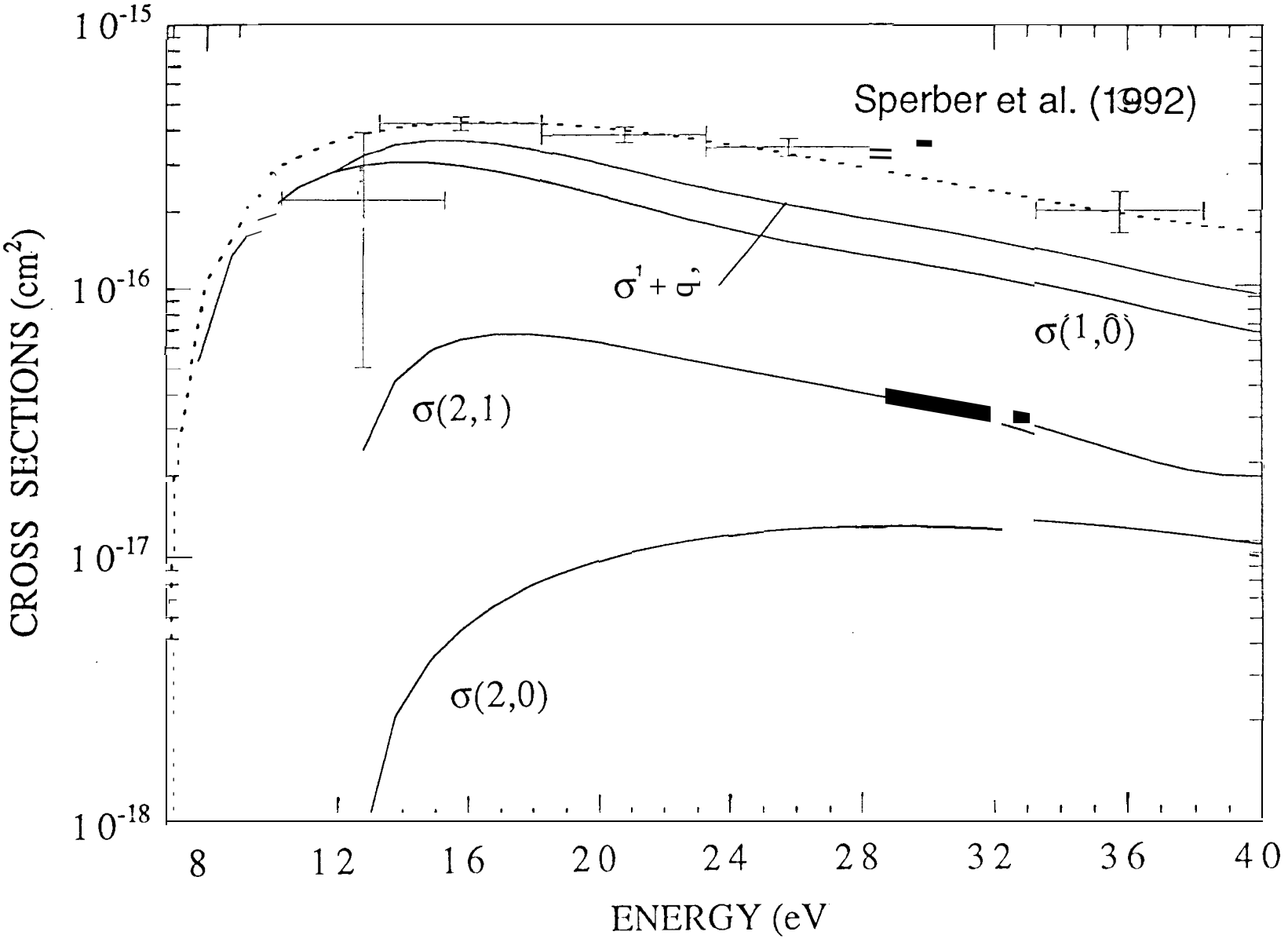
Sperber et al. (1992)
σ¹ + q₂
σ(1,0)
σ(2,1)
σ(2,0)
CROSS SECTIONS (cm²)
10⁻¹⁵
10⁻¹⁶
10⁻¹⁷
10⁻¹⁸
8
12
16
20
24
28
32
36
40
ENERGY (eV

FIGURE 8

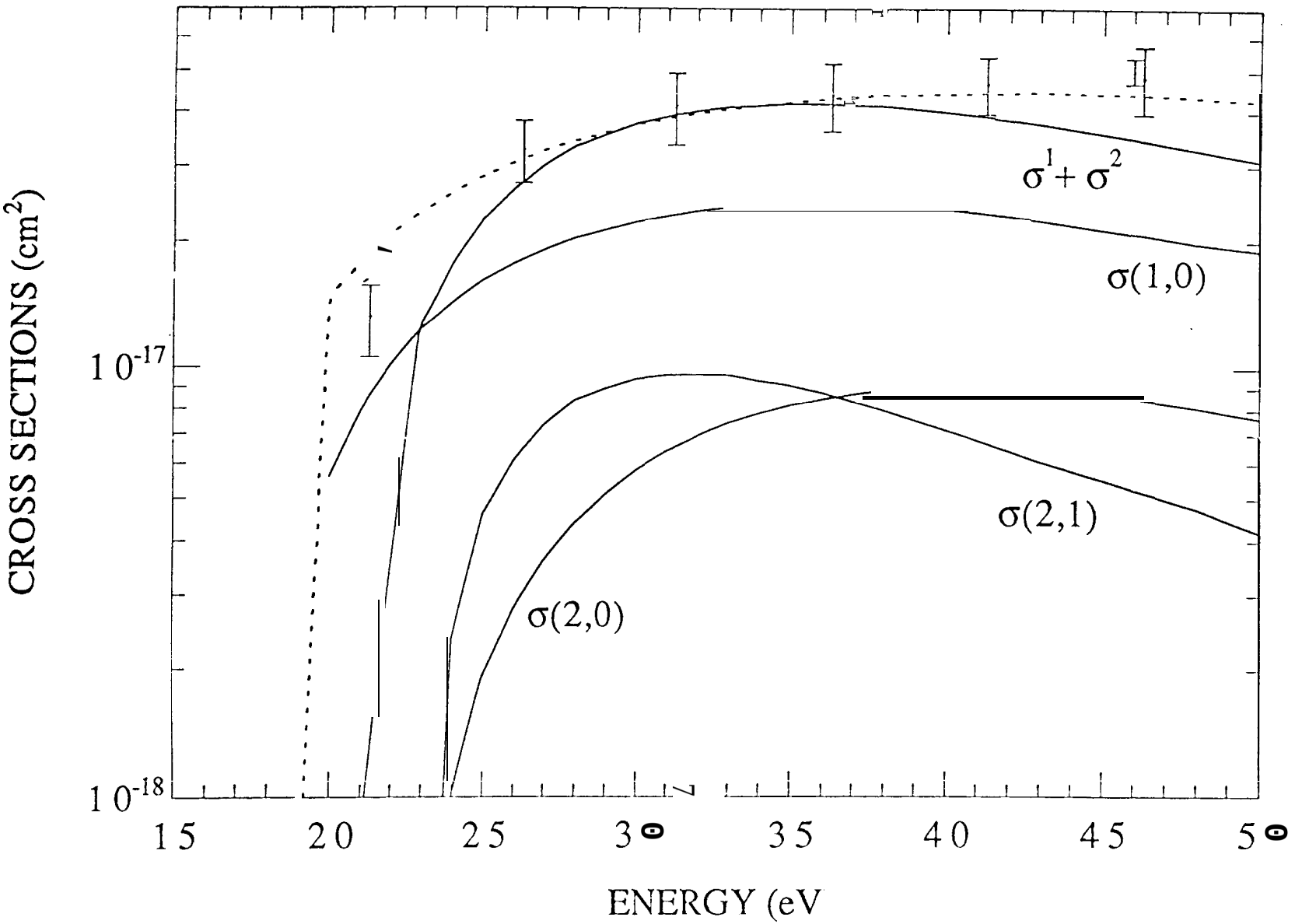
CROSS SECTIONS (cm^2)
10^{-17}
10^{-18}
$\sigma^1+\sigma^2$
σ(1,0)
σ(2,1)
σ(2,0)
15
20
25
30
35
40
45
50
ENERGY (eV

FIGURE 9

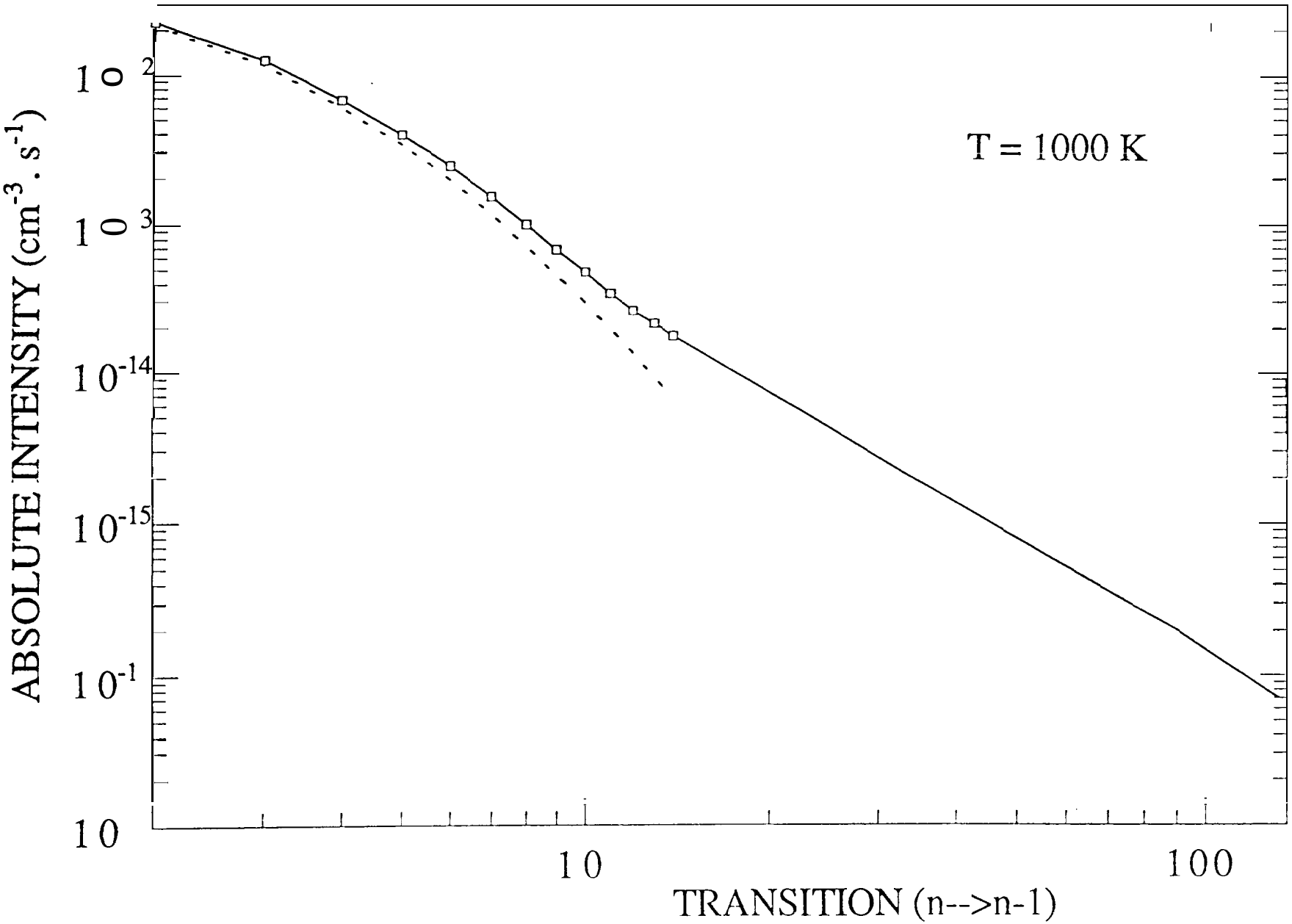
ABSOLUTE INTENSITY (cm-3 . s-1)
10 2
10 3
10-14
10-15
10-1
10
10
100
TRANSITION (n-->n-1)
T = 1000 K

FIGURE 8

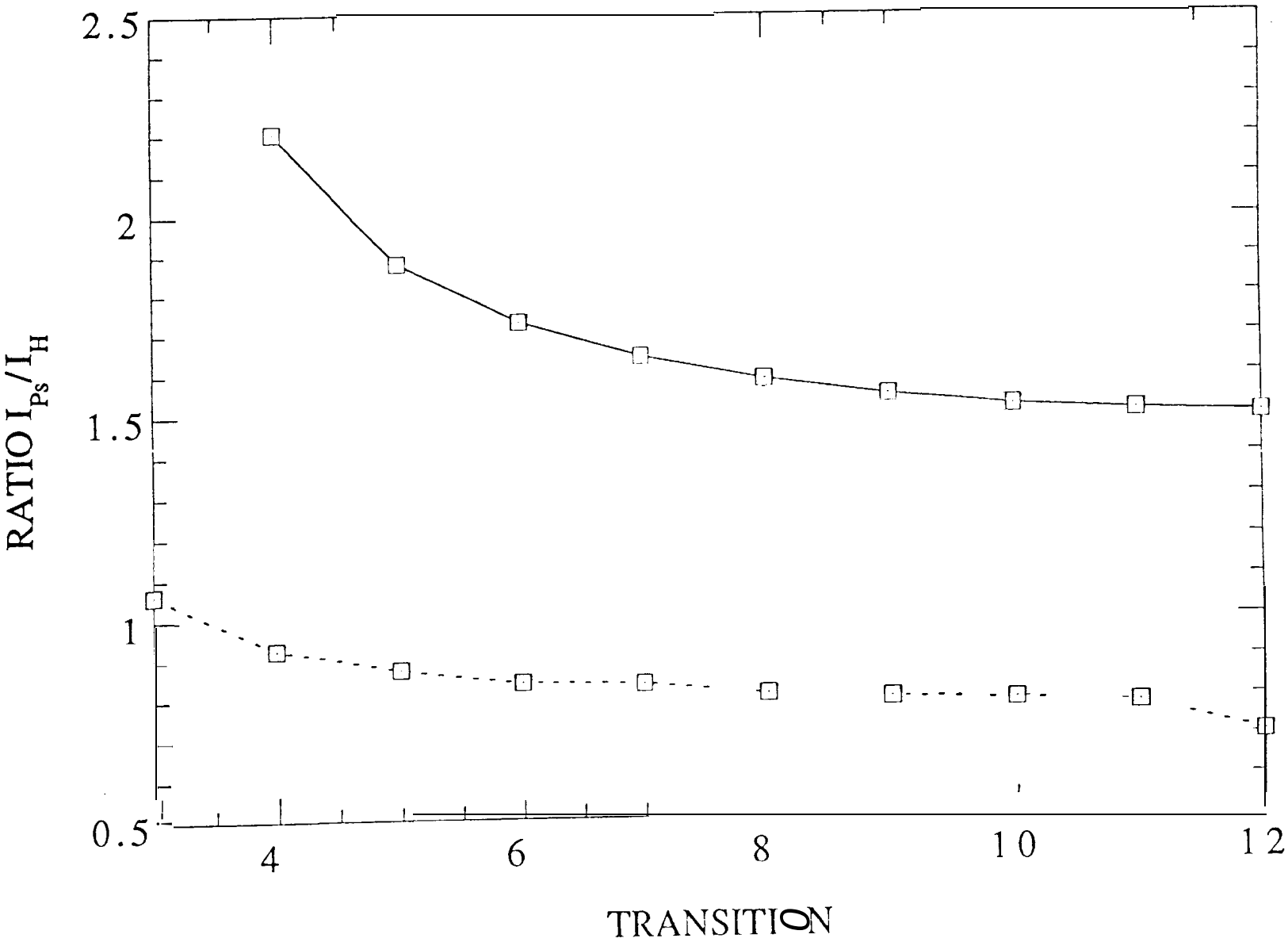

FIGURE 11

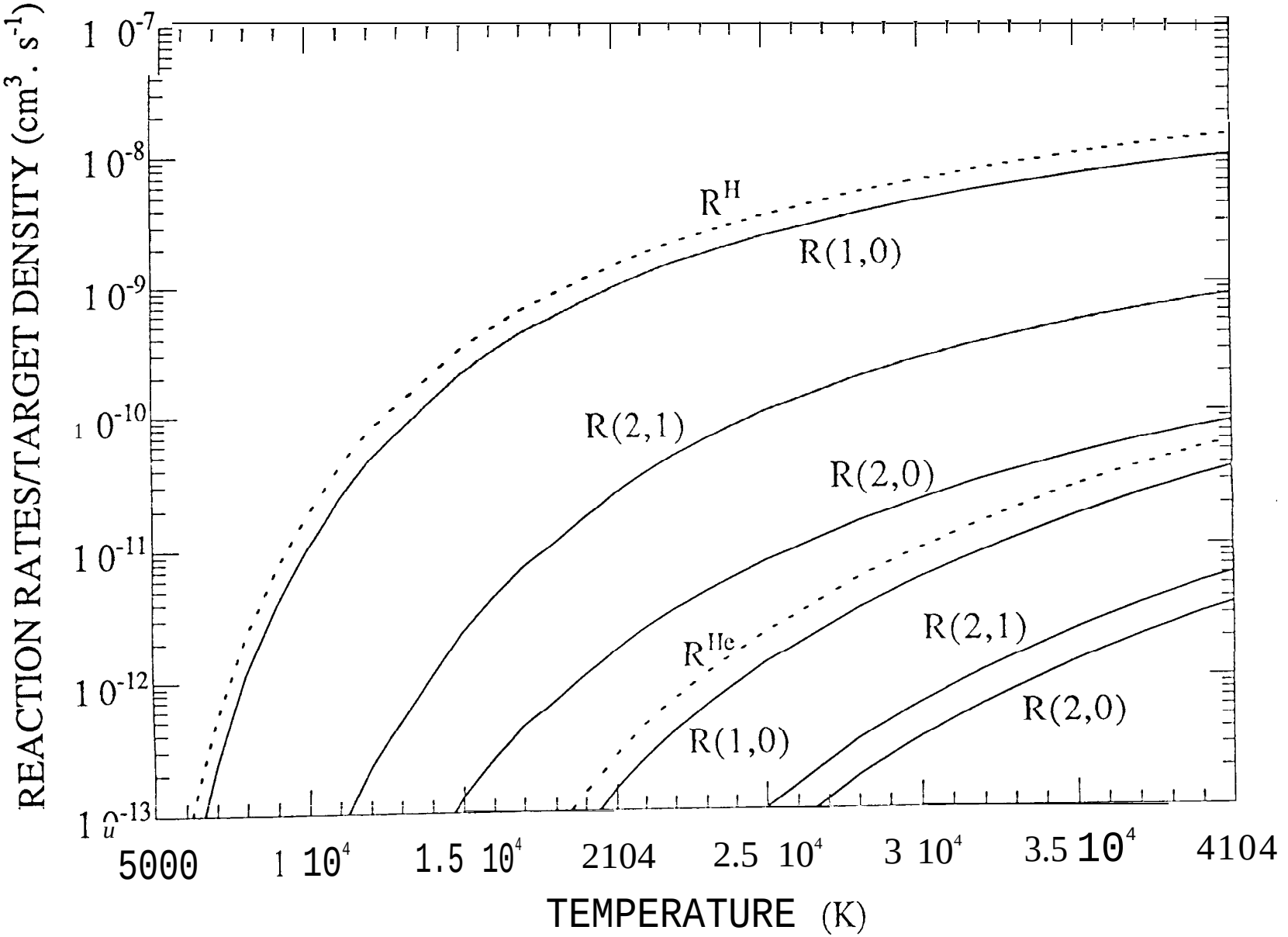
REACTION RATES/TARGET DENSITY (cm^3. s^{-1})
1 0^{-7}
1 0^{-8}
1 0^{-9}
1 0^{-10}
1 0^{-11}
1 0^{-12}
1 0^{-13}
R^H
R(1,0)
R(2,1)
R(2,0)
R^{He}
R(2,1)
R(2,0)
R(1,0)
5000
1 10^4
1.5 10^4
2104
2.5 10^4
3 10^4
3.5 10^4
4104
TEMPERATURE (K)

FIGURE 12

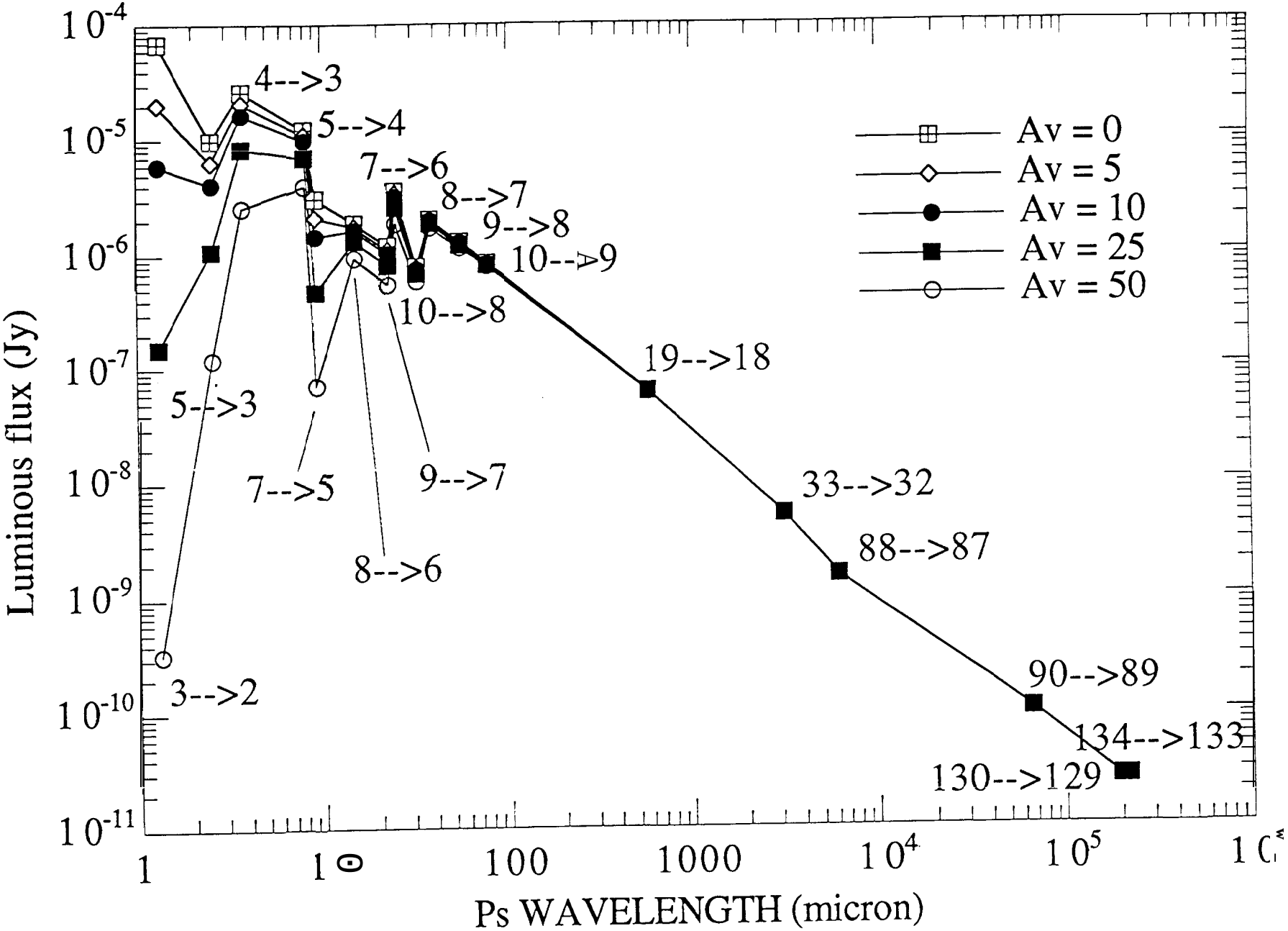
Luminous flux (Jy)
Ps WAVELENGTH (micron)
Av = 0
Av = 5
Av = 10
Av = 25
Av = 50
4-->3
5-->4
7-->6
8-->7
9-->8
10-->9
10-->8
19-->18
5-->3
7-->5
9-->7
33-->32
8-->6
88-->87
90-->89
134-->133
130-->129
3-->2